Kinetic model for ye'elimite polymorphs formation during clinkering production of CSA cement

Ariel Berrio[1,2], Jorge I. Tobón[1*], A.G. De la Torre[3]

1. Cement and Building Materials Research Group. Department of Materials and Minerals. Universidad Nacional de Colombia. Colombia.
2. Research and Development Group Cementos ARGOS S.A
3. Departamento de Química Inorgánica, Universidad de Málaga, Campus Teatinos S/N. 29071-Málaga, Spain

Abstract

The calcium sulfoaluminate, orthorhombic (OY) and pseudo- cubic (CY) ye'elimite polymorphs, were synthesized by solid state reaction from SiO_2, Al_2O_3, Fe_2O_3, $CaCO_3$, Na_2CO_3, $CaSO_4.2H_2O$ in specific oxide relationships. Thermal gravimetric analysis (TGA) was made before sintering the raw mixes in an electrical furnace. Laboratory X-Ray Powder Diffraction (LXRPD) and Rietveld quantitative phase analysis (RQPA) and amorphous and crystalline non-quantified (ACn) quantification were made on each sample. Kinetic were analyzed isothermally between 1150°C and 1300°C. The kinetic model who best fitted each OY and CY polymorph was the geometrical and diffusional model proposed by Jander (D3 model). The activation energy, Ea (kJ/mol), values obtained for OY and CY were 420 and 275 respectively. The activation energy is lower in CY due to the presence of minor elements that reduce the sintering temperature. The frequency factor or compensation factor A is higher for OY than CY, meaning the need for a higher collision frequency. As founded by previous authors, the coexistence of both polymorphs must be considered into the kinetic study as a fundamental condition of these results. For this reason, this research proposes the inclusion of $\alpha_{modified}$. OY always is present at the reaction beginning. But as higher the temperature and reaction time, in the presence of some minor elements, CY appears mainly at lower temperatures regarding OY, it means requiring lesser energy. Knowing the kinetic model proposed by this work would allow a better control or tailor of the ratio OY/CY, to produce CSA with different performances.

Keywords: CSA cement, pseudo cubic Ye′elimite, orthorhombic Ye′elimite, polymorph Ye′elimite, kinetic CSA cement.

1. Introduction

CSA, calcium sulfoaluminate, cements have been widely studied by scientists and industrial level cement producers [1]–[3][4] since the 70s. Particularly, during the last decade, the studies have been deeper and more specialized in aspects of the crystalline structure, hydration kinetics, among others CSA chemical, physical and mineralogical characteristics. Due to the benefits and advantages associated with the lower energy required for its production and lower CO_2 emissions of CSA cement (~35%) in comparison to Portland Cement (PC) [5] and its adaptability to the modern industrial cement process production [6][7][8] , this cement has been considered as a low CO_2 cement and it has been included into the cement portfolio of different industrial producer , with high interest on the impact from both the environmental and functional point of view of this kind of cement[10]. Due to

Corresponding author: *Jorge I. Tobón. E-mail: jitobon@unal.edu.co

those potential characteristics this cement has been known under the generic name of "third cement series" [11], as an alternative for Portland cement[12][13].

On the other hand, it is important to highlight that the research carried out by different scientists have strongly focused their work on both the mineralogical composition of CSA cements and the effects on the hydration process as well [6][14][9]. Furthermore, some hydration aspects regarding the crystalline composition in CSA cement have been studied [14][15], particularly how the crystalline compound called ye'elimite, as the main phase of CSA cement, features different hydration kinetics if compared to PC crystalline compounds [16] and consequently differences over their hydration kinetics and mechanical performances. Ye′elimite remarkably shows some advantages on its hydration speed which are associated with the high early strength reached by this kind of materials and also its faster setting time [17][18][19]. These features encourage researchers to investigate even more and understand the CSA cement characteristics and how to improve the CSA cement production process by using different raw materials widely available in the world [6][20]. Those characteristics can attract the concrete end-users of cement to use it as a new product with better performance at early ages (precast, pavements, others). Due to its potential uses, the relevance of the scaling production process of CSA from laboratory to industrial, adapting and using the same Portland cement installations, it becomes even more interesting [21][22]. The importance of looking after the chemical formulation balance between alumina and silica in order to control the quality of CSA clinker is relevant due to the inhibition reactions occurring during the ye'elimite formation [23]. Depending on the silica content it can promote the formation of other crystalline compounds during the CSA clinker process, like gehlenite, which competes with ye'elimite [24] during the solid to solid reactions in a kiln. By controlling the ye'elimite formation, overcoming the competitive reaction, there is another challenge regarding the different ye'elimite crystalline structures, which analogically to PC main compounds polymorphs, they give to CSA cement various performance in terms of hydration kinetics. Pseudo-cubic ye'limite as a transition phase and the lowest energy structure orthorhombic ye'elimite, behaves different during hydration process. This work focuses in describing the kinetics of the solid-state chemical reaction as occurs in CSA cement production (as an industrial scale) [25] by differentiating the well known polymorphs (pseudo-cubic and orthorhombic).

Solid-state kinetic models have been used for describing the sintering process of clinker cement, which occurs in a rotary kiln, where reactions between crystal lattices as function of lattice defects predominate [26]. For many years to nowadays, kinetic data has been collected to describe ye'elimite formation, by using a theoretical-mathematical description model which represents what occurs in the reaction [27]–[29]. A combination between geometrical contraction and diffusional models (D models, D1, D2, D3 and D4 models [30]) represent a very well description of both ye'elimite kinetics, this model have been found in other references [31][32]. The expression for D3, Jander's model, for a spherical particle is:

$$(1 - (1 - \alpha)^{\frac{1}{3}})^2 = k't \quad (1)$$

Where α stands for the conversion factor, k' is k/R^2 (k: rate constant; R: radius of the spherical particle) and t, is time, in seconds.

The deacceleration reaction rate due to the particle contraction and the tortuosity formed in the same particle due to the decarbonation could be well represented by the combined model. The solid-state polymorphic transition of ye'elimite from orthorhombic to pseudo-cubic is a phenomenon that has the same kinetic principle, from the phenomenological point of view. In each CSA cements around the world, ye'elimite is present in different polymorphs' proportions. To develop this work, it is necessary to consider as a simplification on crystalline synthesis for the mathematical model, that is both, orthorhombic and pseudo-cubic (hereinafter it will be called just cubic ye'elimite) ye'elimite

Corresponding author: *Jorge I. Tobón. E-mail: jitobon@unal.edu.co

will be synthetized separately, by considering the sintering process given by [33], but, it is clearly identified the coexistence of both polymorphs in CSA clinker synthetized, the refine structure given by [33] represents a very good approximation of each ye'elimite, for the purpose of this research. Particularly the referred approximation describes the crystalline presence and confirms both polymorphs can be described by a similar kinetic mathematic model.

Furthermore, some assumptions must be necessary to define a kinetic model to represent the kinetic behavior of ye'elimite synthesis. According to [34] to use the Jander's model it is assumed that (1) the diffusion of CaO through the melt is the rate-controlling reaction; (2) the diffusion coefficient for CaO is constant and independent on the concentration in the actual system; (3) the original contact face between the CaO particle and the clinker is maintained during reaction; i.e. the original diffusion surface of CaO is constant with time (the particle diameter is constant); (4) the stationary spherical diffusion field can be applied; (5) the amount of liquid phase is constant through the reaction zone; (6) the densities of the different liquid systems are equal; and (7) the reaction zone is pore-free regardless of the porosity of the clinker.

The control of the polymorphic formation in CSA cement production will yield to tailored-made final CSA cement performances. The main goal of this work is to describe the kinetics of each polymorph formation (finding the main kinetic parameters), since there is a lack of information on this issue. The final objective is to be able to control the formation of one polymorph over the other one to bias the performances in CSA cement.

Therefore, the contribution in this research around the formulation of a kinetic model allows describing the formation reaction of the different polymorphs of the compound ye'elimite, orthorhombic and pseudo-cubic, as main phases of calcium sulfoaluminate cement based (CSA). By knowing the kinetic of each polymorph and the main parameters that describe it, such as activation energy, frequency factor or speed constants, it is possible to tailor the production of a CSA cement with an established proportion of each polymorph. This knowledge will yield to achieve a suitable CSA cement with tailored hydraulic properties.

2. Materials and Methods

2.2 Materials and samples preparation

Ye'elimite polymorphs were synthesized from analytical grade oxides, which are listed in **¡Error! No se encuentra el origen de la referencia.**. The oxides were mixed and pre-homogenized in a laboratory mixer, a micro-Deval machine (A0655, Proeti S.A., Spain) during 1 hour at 100 rpm with steel balls (2 balls of 20 mm diameter and 2 of balls of 10 mm diameter). Ye'elimite samples were synthesized following the methodology published by Cuesta et al. [33], [35].

Table 1. Chemical compounds used for ye'elimite synthesis (orthorhombic ye'elimite: OY; cubic ye'elimite: CY) and dosing of each raw mixture.

Compound	Trademark	Purity/%	Polymorphism	OY (g)	CY (g)
SiO_2	Alfa Aesar	99.500	Amorphous	-	3.9583
Al_2O_3	Alfa Aesar	99.997	α-γ Al_2O_3	100.2511	93.5677
Fe_2O_3	Alfa Aesar	99.945	Hexagonal	-	5.2363
$CaCO_3$	Alfa Aesar	99.990	Calcite-Aragonite	98.4149	91.8534
Na_2CO_3	Aldrich	99.999	Orthorhombic	-	3.4752
$CaSO_4.2H_2O$	Alfa Aesar	98.000	Monoclinic	57.5777	57.5781
Total amount				**256.2437**	**255.6690**

Corresponding author: *Jorge I. Tobón. E-mail: jitobon@unal.edu.co

Two raw mixtures (approximately 255 g each, Table 1) were prepared for stoichiometric ye'elimite, called hereafter OY and doped ye'elimite, called hereafter CY. A mixture of $CaCO_3$, Al_2O_3 and $CaSO_4 2H_2O$ (3:3:1 molar ratio) for OY and a mixture of $CaCO_3$, Al_2O_3, $CaSO_4 2H_2O$, Fe_2O_3, Na_2CO_3 and SiO_2 (2.8:2.8:1:0.2:0.2:0.2 molar ratio) for CY were prepared. Both OY and CY raw materials were accurately weighed and homogenized for 1 hour in the micro-Deval machine (as described before). After mixture homogenization, the raw mix was moistened (15 wt.% isopropanol) until a workable and consistent paste was obtained in such a way that pellets could be made in disk pellets (20 mm of diameter and 3 mm thick, 1.5 grams each pellet). The disk pellets were made for each mixture by uniaxial pressing using at steel die (press loading of 0.05 MPa for 1 minute each pellet).

Both polymorphs raw material pellets were thermally treated. Pellets were heated in a laboratory furnace, with a heating rate of 15 °C/min up to 900°C, then it was left at this temperature for 30 minutes to ensure decarbonation. Then, heating was continued at 10 °C/min up to the final temperature (1300 or 1250°C, for OY and CY, respectively) and held there for 45 minutes, those temperatures were found on previous works [33]. The residence time was chosen based on previous research [36] and in analogy to the industrial production, where most of the modern industrial kilns uses around 30 min or less, to burn the raw mix. This time was also referred in previous research work [21], this 45 minutes make sure the ye'elimite formation avoiding sulfur volatilization [37]. After this burning process, the material was cooled to room temperature by forced air.

2.3 Methods

2.2.1. Thermal treatments.

Both raw mixtures were sintered at different temperatures to follow the mechanisms of formation. Due to the nature of each polymorph, different oxides were used as was explained above to guarantee each polymorph stabilization. Both raw mixtures were sintered from 1000 to 1300 ºC in steps of 50 ºC. The residence time at each temperature was 4 hours. On the other hand, for kinetic evaluation, the raw mixtures were heated at selected temperatures by using different residence times ranging from no residence time to 6 hours, covering from the induction period up to full reaction.

2.2.2. Laboratory X-Ray Powder Diffraction (LXRPD)

Corresponding author: *Jorge I. Tobón. E-mail: jitobon@unal.edu.co

Powder patterns for the samples treated at different temperatures and times of residence were recorded on a D8 ADVANCE from Bruker AXS (Germany) diffractometer, placed at SCAI at University of Malaga (Spain), using monochromatic $MoK_{\alpha 1}$ radiation (λ = 0.7093 Å) provided by a Ge (111) primary monochromator and with LYNXEYE XE 500 μm linear dispersive energy detector, optimized for high-energy radiation, with the maximum opening angle. The samples were placed between kapton foils to be measured on transmission geometry and were rotated at 10 rpm during data collection. Data were collected from 3º to 35° (Mo-2θ) with a total time per pattern of 28.8 minutes. For the identification of the mineralogical phases in each pattern, the High Score Plus software and the ICSD 2011 database were used. Quartz (99.56%, ABCR GmbH & Co. KG) was used in a ~20 wt.% as internal standard on each sample in order to determine the ACn content [38].
High temperature (HT) LXRPD studies were carried out in a PANalytical diffractometer, X'Pert MPD PRO model. A strictly monochromatic $CuK_{\alpha 1}$ radiation (λ=1.54059 Å) provided by a Ge (111) primary Johansson monochromator was used and a X'Celerator RTMS (Real Time Multiple Strip) detector, working in scanning mode with maximum active length. An Anton Paar HTK1200 camera under static air was used to perform the high temperature LXRPD study. The mixes were warmed up from room temperature (RT) to 900°C, after that a delay of 15 min at 900°C to ensure the sample thermal equilibrium were acquired over the angular range 5−70° (2θ) with a step size of 0.017°, resulting in a 47 min acquisition time per pattern. XRD data were collected in a temperature range between 900 to 1200°C, with temperature intervals of 50°C. The sample was then in-situ cooled to RT where a final LXRPD pattern was acquired.

2.2.3. Rietveld quantitative phase analysis (RQPA) and Amorphous and crystalline non-quantified (ACn) quantification

The patterns were analyzed by direct Rietveld method using GSAS [39] software by using a pseudo-Voigt peak shape function with asymmetry correction included [40], [41], to obtain RQPA. The refined overall parameters were: phase scale factors, background coefficients, unit cell parameters, zero-shift error, peak shape parameter, and preferred orientation coefficient, if needed (March-Dollase ellipsoidal preferred orientation correction algorithm [42]). The ACn content was determined by the internal standard method [38].

2.2.4. Scanning electron microscopy (SEM) analysis.

Cross-sections of selected samples (CY_1250C_4h and OY_1300C_4h) were performed in a JEOL JMS-6490LV scanning electron microscope using secondary electrons at 15 kV, to study the microstructure. Prior to SEM observation, the sample was gold coated (by sputtering during 10 min until obtain a 30 nm coating thickness) to improve the conductivity of the sample and the quality of the images.

2.2.5. Specific Surface area measurement

The specific surface area of anhydrous samples was also carried out by BET (Brunauer-Emmett-Teller) methodology. These measurements were performed in an automatic equipment MICROMERITICS ASAP 2020 (supplied by Micromeritics Instrument Corporation, USA). Isotherms at low partial pressure of an inert gas (N_2, at room temperature) were used to determine specific surface area. The total surface area of the powders was calculated using the Langmuir theory ant the BET generalization. Usually, the BET method gives the results two or three times higher that air permeability method (or Blaine method), because it includes internal surfaces present in micro-cracks or in pores open at only one end [43].

Corresponding author: *Jorge I. Tobón. E-mail: jitobon@unal.edu.co

2.2.6. Particle Size Distribution (PSD).

The particle size distribution of the powders was measured by laser diffraction in a wet chamber by suspending in isopropanol using Malvern Master Sizer S (from UK). Each sample was dispersed previously in isopropanol in test tubes using an ultrasonic bath.

2.2.7. Isothermal micro-calorimetry

TAM Air Isothermal conduction micro-calorimeter (TA Instruments, USA) was used to study the heat flow emission from hydration reactions at 25°C for 48 hours with water/cement ratio (w/c) ranging from 0.75 to 1.10. Since these samples' hydration is very fast, an admix tool was used to mix 2 g of anhydrous samples and the corresponding amount of water inside the micro-calorimeter for 2 minutes, to avoid any data loss. In the reference vessel, a sample of PC was placed (2 g), due to its similar heat capacity. The reference vessel is used to reduce the signal-to-noise ratio and to correct both measurement and temperature device. The temperature of each channel was stabilized 24 hours before any experiment.

2.2.8. Differential Scanning calorimetry and thermogravimetric analysis (DSC-TGA)

DSC-TGA studies were performed on raw mixtures. DSC-TGA were carried out in an SDT-Q600 analyzer from TA Instruments (New Castle, DE) under dry air atmosphere (flow rate 100 mL/min), over temperature range of 20-1000°C with a heating rate of 10 °C/min. Open platinum crucibles were used, and the sample weight was approximately 40 mg. Data were processed using TA Instruments Universal Analysis 2000.

3. RESULTS AND DISCUSSION

3.1. Particle size distribution:

Particle size distribution represents a basic condition for reaction kinetic process. Control of PSD is fundamental to understand the reaction process. Figure 1 and Figure 2 show the particle size distribution (PSD) of the raw materials and mixtures and the final samples prepared in this study, respectively. BET values for the final OY and CY were 2.34(1) and 2.69(2) m^2/g, respectively.

Corresponding author: *Jorge I. Tobón. E-mail: jitobon@unal.edu.co

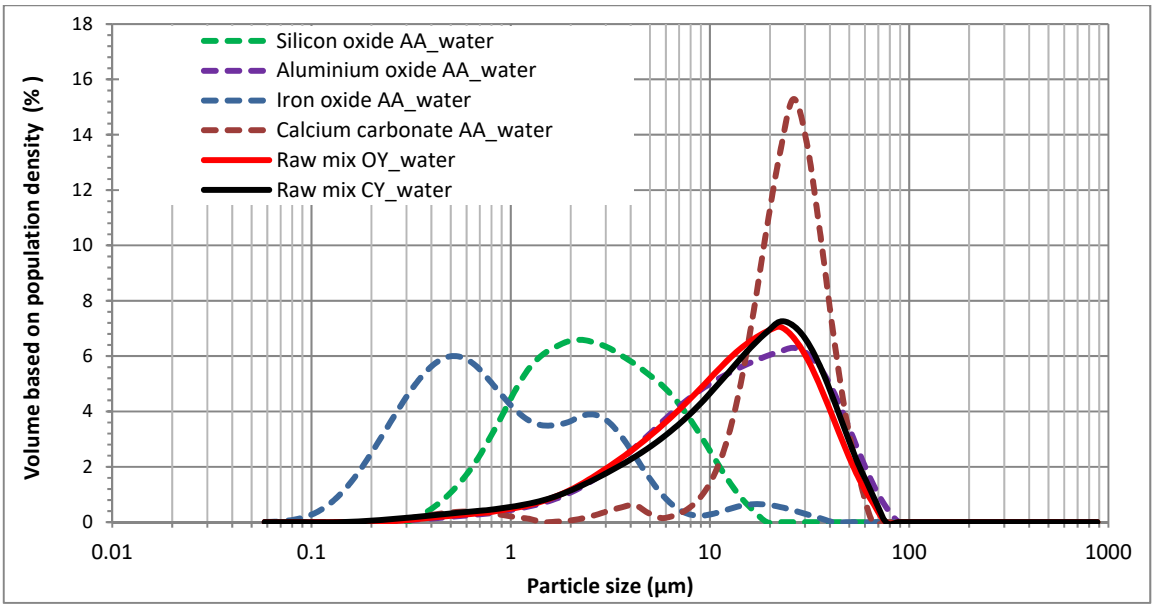

Figure 1. Raw materials and raw mixtures PSD. Reagent grade chemical SiO_2, Al_2O_3, Fe_2O_3 and $CaCO_3$ Alfa Aesar (AA) were analyzed in water as medium, idem for raw mix_OY and raw mix_CY.

It is noticeable that the PSD of both OY and CY raw mixtures are similar.

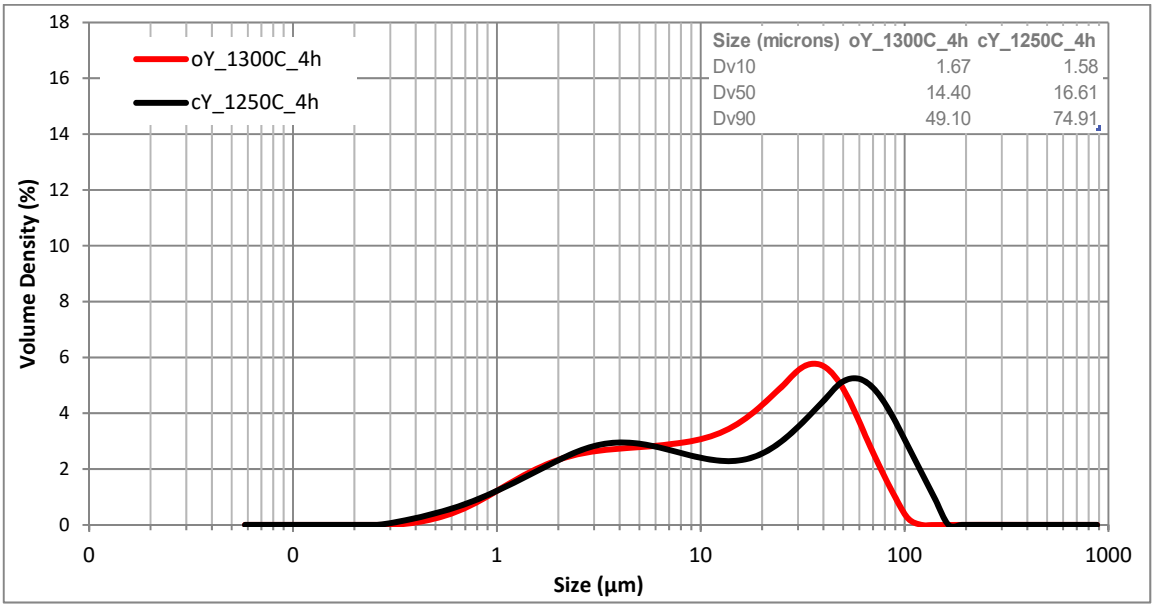

Figure 2. PSD of final ye'elimite polymorphs.

After clinkering both raw mixtures up to 1300ºC and 1250ºC for OY and CY, respectively for 4 hours, the samples were ground with the same procedure, giving the PSD displayed in Figure 2. The specific surface area of anhydrous samples was carried out by BET, values agree with PSD, being OY slightly finer than CY. For CY, BET Surface Area obtained was 2.3411 ± 0.0111 m^2/g and for OY, BET Surface Area obtained was 2.6886 ± 0.0178 m^2/g.

3.2. Thermal analysis:

Figure 3. gives DTA-TGA curves of OY and CY raw mixtures treated up to 1300°C, respectively.

Corresponding author: *Jorge I. Tobón. E-mail: jitobon@unal.edu.co

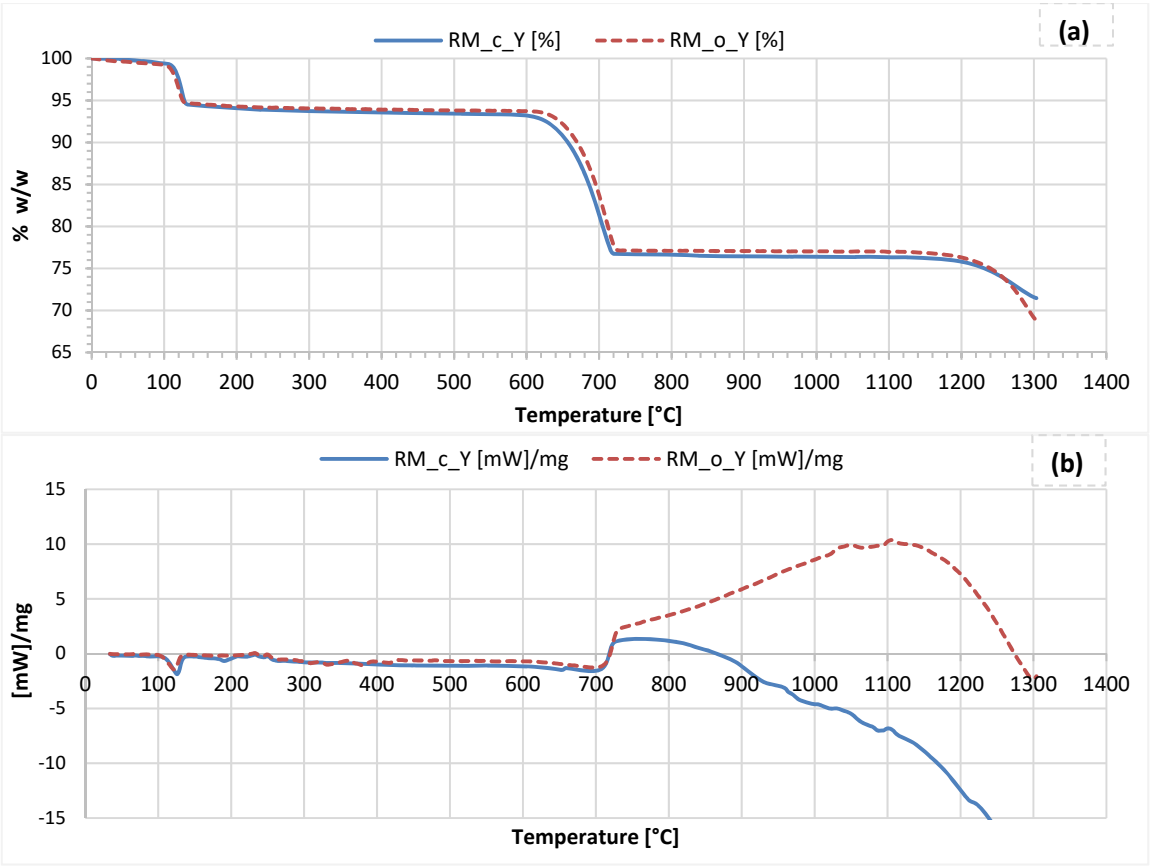

Figure 3. (a) TG and (b) DSC for orthorhombic (RM_o_Y) and cubic (RM_c_Y) ye'elimite raw mixtures.

It is observed from Figure 3 that both raw materials have a very similar loss of weight when temperature is increased. Dehydration of gypsum (~120ºC), decarbonation (~700ºC) and clinkering processes (~1200ºC) take place in these temperature ranges, Figure 3(a). Both raw mixtures show a loss weight from 1200ºC, which may be associated with a partial decomposition of ye'elemite loosing SO_3 [28] According to the DSC given in Figure 3 (b), the energy required for OY synthesis is higher than for CY, since a higher endothermic transition is observed in OY starting from 700°C associated with decarbonation process, another phase transition takes place above 900°C, where OY demands more energy flux during the transition to become ye'elimite compare to CY. These data agree with the higher temperature require to obtain OY.

3.3. Ye'elimite formation results

Mineralogical analysis of the OY and CY: ¡Error! No se encuentra el origen de la referencia. *and Figure* S2, given as supplementary information, show the LXRPD patterns of synthesized OY at 1300°C *and* of CY at 1250°C, respectively, with different dwelling times. Table 2 and Table 3 summarizes the RQPA analysis of all the samples prepared with OY and CY raw mixtures, respectively, and includes the ACn content calculated by the internal standard method [26]. The increase in the time of residence at high temperature enables the formation of higher amounts of ye'elimite (OY or CY) content, which is quantitatively given in Table 2 and Table 3 and observed in Figures S1 and S2, by analyzing the intensity ratio between the main diffraction peak of ye'elimite placed at $2\theta_{Mo}$=10.8º and that of quartz at $2\theta_{Mo}$=12.2º. Analyzing these data, it can be stated that

Corresponding author: *Jorge I. Tobón. E-mail: jitobon@unal.edu.co

1300ºC and 1250ºC and 4 hours of dwelling are the proper conditions to complete both OY and CY formation, respectively.

Table 2. RQPA, in weight percentage, for OY raw mixture at 1300°C at different dwelling times.

Phase	OY_1300C_0h/wt.%	OY_1300C_15min/wt.%	OY_1300C_90min/wt.%	OY_1300C_4h/wt.%
o_$C_4A_3\bar{S}$	44.9 (2)	90.6 (1)	94.6 (1)	97.2(1)
$C_{12}A_7$	6.1 (2)	2.4 (1)	0.6 (1)	-
CA_2	5.7 (4)	-	0.2 (1)	-
CA	7.1 (3)	0.5 (2)	0.9 (2)	0.8(2)
$CaSO_4$	12.9 (2)	2.1 (2)	0.4 (1)	0.4(2)
$Ca(OH)_2$	6.4 (2)	0.3 (2)	1.4 (2)	0.2(2)
CaO	1.2 (1)	0.2 (1)	0.1 (1)	0.9(2)
Al_2O_3	15.3 (2)	1.8 (1)	0.6 (1)	0.5(2)
ACn	0.4	2.3	1.2	0.0

During the first 15 min, nonreacted components, i.e., $CaSO_4$, and intermediate phases, $C_{12}A_7$, CA_2 and CA are present in the final product and some partial hydration of free lime is noticed due to de short contact with the humidity of the atmospheric air during sample grinding. Table 2 shows that for the synthesis of OY at 1300°C, 15 minutes at high temperature is time enough to reduce the intermediate phases and to almost complete the reaction formation, since the free lime is reduced significantly. The kinetics of OY can be represented by the typical diffusion controlled reaction model, as suggested by different authors [44][27][28].

Table 3. RQPA, in weight percentage, for CY raw mixture at 1250°C at different dwelling times.

Phase	CY_1250C_0h/ wt.%	CY_1250C_15min/ wt.%	CY_1250C_2h/ wt.%	CY_1250C_4h/ wt.%	CY_1250C_6h/ wt.%
c_$C_4A_3\bar{S}$	29.9 (10)	42.8 (8)	54.0 (7)	62.1 (6)	67.6(5)
o_$C_4A_3\bar{S}$	42.0 (8)	38.9 (8)	35.6 (8)	29.0 (9)	24.0 (9)
$C_{12}A_7$	1.6 (2)	-	1.0 (2)	-	-
CA	7.0 (4)	3.7 (2)	2.3 (3)	3.3 (3)	2.2 (2)
$CaSO_4$	4.7 (2)	2.2 (1)	-	-	-
CA_2	3.4 (4)	3.8 (5)	3.4 (2)	1.0 (1)	1.4 (2)
C_2S	1.3 (2)	1.7 (2)	2.2 (3)	-	2.4 (2)
ACn	10.1	6.8	1.5	4.6	2.3

Dopants were introduced in the raw mixture in order to obtain the pseudo-cubic polymorph of ye'elimite, since the substitutions of mainly Ca^{2+} by Na^{+} and Al^{+3} by Si^{4+} or Fe^{3+} enables to restore the pseudo-cubic symmetry [45]. The polymorphism of solid solution ye'elimite has been investigated in the past [46] [47] [48] showing that the dopants provokes a dynamical disordering of the sulfate anions within the cages [35]. Moreover, due to the impossibility of having a crystal structure description for each member of the solid solution, $Ca_{4-2y}Na_{2y}Al_{6-2x}Fe_{2x}SO_{16}$, the best approach to perform quantitative phase analysis is to use both published crystal structures, i.e. orthorhombic and pseudo-cubic, in order to simulate this doped ye'elimite [49]. Consequently, to perform RQPA in the CY raw mixtures thermally treated at 1250ºC and at different dwelling times, both polymorphs have been used, Table 3. It is noticeable that the amount of CY increases with the increase of residence time as expected.

As mentioned above some additional phases are present in the CY synthesis, as well as in OY synthesis, the main difference is the quantity of those ones. Free lime is no detected at any time of clinkering. The amount of ACn is reduced significantly when the raw material is heated for 2 hours or more. This is mainly due to the enlarging of crystal size and the reduction of crystal strains with longer residence times. RQPA results of the different dwelling times give the clear idea that, as expected, the kinetics of OY and CY depends not only on temperature, but also on residence time and chemical compounds (see Table 2 and Table 3). In addition to the clinkering process, the kinetic model is necessary to describe the CY formation, which will also give information about energy needed to form CY compare to OY.

Corresponding author: *Jorge I. Tobón. E-mail: jitobon@unal.edu.co

It is highlighted also (Table 2 and Table 3) the presence of cubic and orthorhombic ye'elimite but not crystalline compounds (like gehlenite) due to the lower SiO_2 content, as described by [36]. It is important to emphasize that the problem of the exclusion between these two phases (gehlenite and ye'elimite) and their strong dependence with the Al_2O_3/SiO_2 ratio is not a real problem using reagent compounds and lower quantities of SiO_2 [36]. It is also important to emphasize that in the case of 1250ºC and 1300ºC the pure phase presents nothing of gehlenite and higher ye'elimite, which is highly desired because gehlenite has not hydraulic activity and it affects negatively the mechanical performance as well as the durability of these CSA cements, as it has been posed by some researchers [50] [11].

3.4. Kinetics

The kinetic model for the formation of ye'elimite polymorphs was reached from different tests. Each polymorph formula was sintered isothermally (1250ºC and 1300ºC for CY and OY, respectively) by changing the residence time. As reaction extends the growing up of CY and OY at the very end synthesis is correlated with a kinetic model base on geometrical and diffusional control of the reaction, the advance of the reaction fits with the model chosen in order to represent the ye'elimite kinetics, (Figure 4 and Figure 5). The obtained model for each CY and OY allows to replicate the synthesis reaction vs time data. Some kinetic parameters have been raised, then the postulation of several kinetic models and then the adjustment and/or the verification of the kinetic model that describes the formation of polymorphs. This work focuses on the sintering reaction as the base of the reaction mechanism, of ye'elimite compounds, by modeling its kinetics based on the diffusional kinetic models, which will be domain process in the kinetic description according to the linearity showed down between the integral reaction equation g(α) versus time.
Jander's model describes the best for kinetics of OY and CY (**¡Error! No se encuentra el origen de la referencia.** and **¡Error! No se encuentra el origen de la referencia.**), based on the diffusion and geometric reactions theories in solid state reactions this model represents how the reactions occurs. In general, the rate of a solid state reaction is built from the conversion factor, α, which comes from a gravimetric measurement (RQPA results given in Table 2 and Table 3), the reaction model is a mathematical model that represents the relation between α and time, $f(\alpha)=d\alpha/dt$, but also temperature (if a non-isothermal reaction takes place in the analysis). The integral reaction model, g(α), is obtained after the integration f(α) as a function of temperature. Best approximation for ye'elimte was obtained from Jander model 3-D diffusion-Jander model as described by equations (1) to (3):

$$\alpha = (m_t-m_0)/(m_f-m_0) \quad (1)$$

$$f(\alpha) = [1 - (1 - \alpha)^{1/3}]^2 \quad (2)$$

$$g(\alpha) = [3(1 - \alpha)^{2/3}]/[2(1 - (1 - \alpha)^{1/3})] \quad (3)$$

where m_t stands for the amount of OY from Table 2 or CY from Table 3 at each residence time, m_f stands for the final amount of OY or CY at the longest residence time and m_0 stands for the initial amount of each OY, CY available when reactions begin (0.0% in this case).

Other temperatures were also studied, i.e., 1250ºC, 1200ºC for the OY raw mixture and 1200ºC and 1150ºC for CY raw mixture. It is highlighted the high linearity of integrated model formula as a function of time for all the studied temperatures, with R^2 close to 1.0, Figure 4**¡Error! No se encuentra el origen de la referencia.** and Figure 5**¡Error! No se encuentra el origen de la referencia.**.

Corresponding author: *Jorge I. Tobón. E-mail: jitobon@unal.edu.co

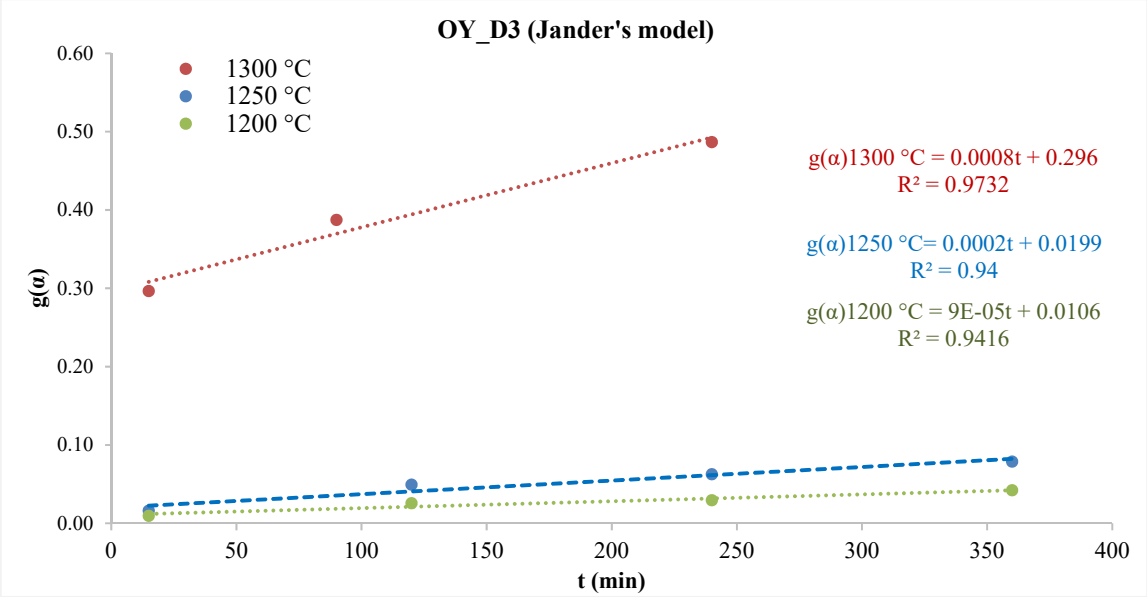

Figure 4. Jander's fitting between g(α) and time (min) of orthorhombic Ye'elimite (OY), Jander diffusivity model, D3.

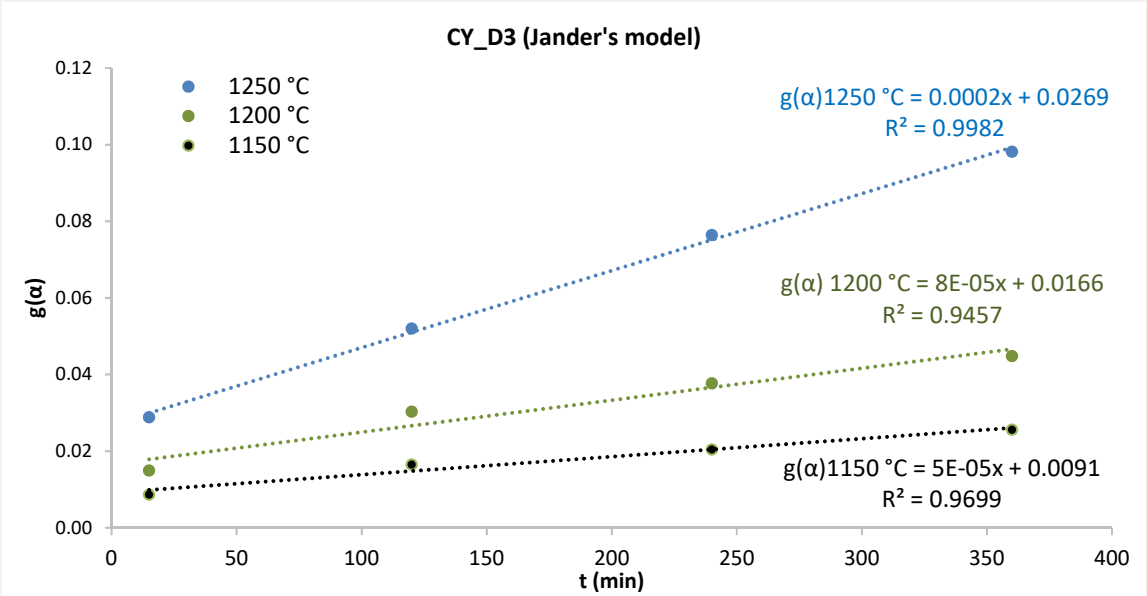

Figure 5. Jander's fitting between g(α) and time (min) of cubic Ye'elimite (CY), Jander diffusivity model, D3.

Furthermore Figure 4 and Figure 5 show the correlations which describes better the ye'elimite kinetic base on the Jander Model D3, diffusion limited, which means a spheric particle of radius r of a component A, the complete surface reacts with component B and developing a reaction product of thickness Y. These figures describe the relationship between the integrated reaction rate g(α) versus time (min). The function g(α) represents the kinetic model selected as representative of the cement clinker production inside a kiln. Due to the significant presence of calcium carbonate inside the reagent compounds (~40 wt.%) the reaction kinetics above 900°C can be described by a model consisting of spherical CaO particles in contact with other solid particles which can be transported across a coherent and adherent layer of reaction product. That layer grows up limiting the particle

Corresponding author: *Jorge I. Tobón. E-mail: jitobon@unal.edu.co

transport or diffusion. There are two phenomena associated to the $CaCO_3$ particles reacting with other particles, the $CaCO_3$ particles release CO_2 above 900°C leaving CaO particles with some porosity [34], the reaction with other compounds occurs thanks to that porosity allowing the layer grow up around the CaO particle changing the shape of the CaO particle and the reaction kinetics.

3.5. Phase changes during clinkering process of OY and CY:

In order to unravel the OY and CY reaction kinetics, different temperatures of synthesis were made in a laboratory furnace at same dwelling time (4 hours). The reagent materials were prepared and calcined at 1000°C, 1100°C, 1200°C, 1250°C and 1300°C for OY; and 1000°C, 1100°C, 1200°C, 1250°C and 1300°C for CY. RQPA was performed, as in section 3.3, for all the samples and the results are presented in Figure 6 and Figure 7.

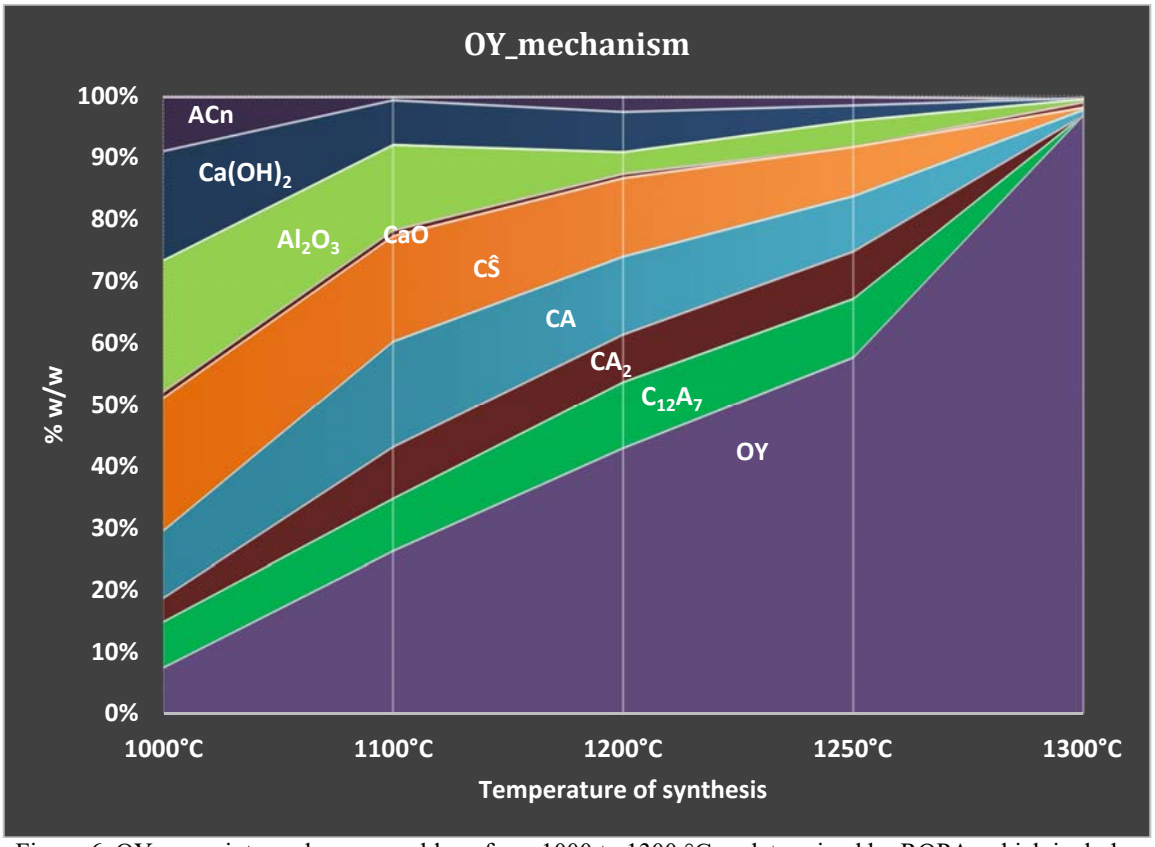

Figure 6. OY raw mixture phase assemblage from 1000 to 1300 °C m determined by RQPA, which includes the ACn content determined by internal standard method.

Corresponding author: *Jorge I. Tobón. E-mail: jitobon@unal.edu.co

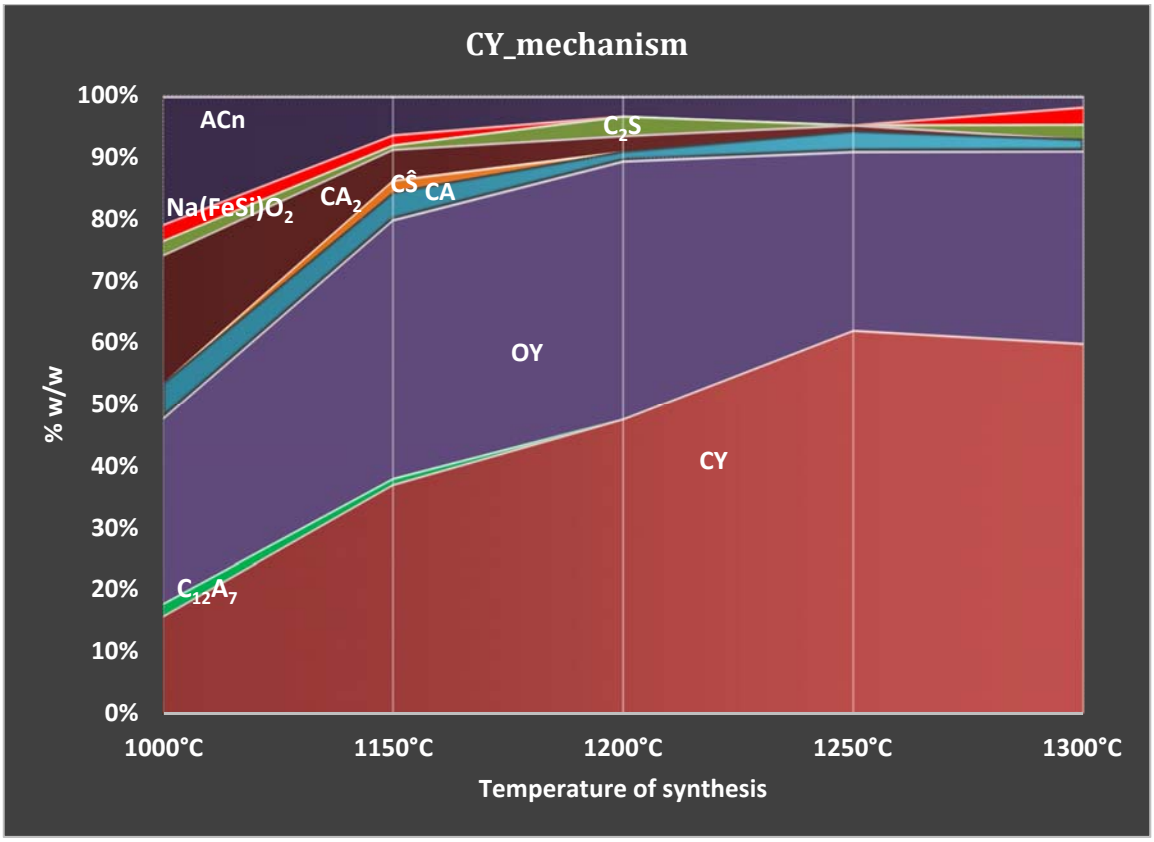

Figure 7. CY raw mixture phase assemblage from 1000 to 1300 °C m determined by RQPA, which includes the ACn content determined by internal standard method.

From Figure 6 it is possible to state that the most feasible mechanism is through solid-to-solid reaction experiment for OY. By assuming that liquid phase is negligible, and the $Ca(OH)_2$ represents the free CaO, that was partially hydrated due to sample manipulation for LXRPD measurements, the following reactions can be proposed:

$$3CaO + Al_2O_3 \xrightarrow{<1000°C} Ca_3Al_2O_6 \quad (4)$$

$$CaO + Al_2O_3 \xrightarrow{1000°C} CaAl_2O_4 \quad (5)$$

$$CaAl_2O_4 + Al_2O_3 \xrightarrow{1000°C} CaAl_4O_7 \quad (6)$$

$$CaAl_4O_7 + 11CaO + 5Al_2O_3 \xrightarrow{1000°C} Ca_{12}Al_{14}O_{33} \quad (7)$$

Reactions (4) to (7) are the formation of different calcium aluminates.

At 1000ºC, OY is already present, the formation of this phase may be proposed the reaction of C_3A with alumina and anhydrite to form ye'elimite, equation (8):

$$Ca_3Al_2O_6 + 2Al_2O_3 + CaSO_4 \xrightarrow{1000°C} Ca_4Al_6SO_{16} \quad (8)$$

As temperature is risen, the remaining aluminates react to form ye'elimite, reactions (9) to (11):

$$3CaAl_2O_4 + CaSO_4 \xrightarrow{>1200°C} Ca_4Al_6SO_{16} \quad (9)$$

Corresponding author: *Jorge I. Tobón. E-mail: jitobon@unal.edu.co

$$\frac{3}{2}CaAl_4O_7 + CaSO_4 + \frac{3}{2}CaO \xrightarrow{>1200°C} Ca_4Al_6SO_{16} \quad (10)$$

$$\frac{3}{12}Ca_{12}Al_{14}O_{33} + CaSO_4 + \frac{15}{12}Al_2O_3 \xrightarrow{>1250°C} Ca_4Al_6SO_{16} \quad (11)$$

Reactions (9) to (11) govern at high temperature, consuming free CaO, alumina and anhydrite.

For cubic ye'elimite, small quantities of Na_2O, Fe_2O_3 and SiO_2 have been added to stabilize this phase, following the methodology reported by Cuesta et al., [35]. The most remarkable difference between the phase evolution of CY and OY with temperature, Figure 6 and Figure 7, is that the amount of ye'elimite (quantified as orthorhombic and cubic) is much larger in CY at 1000ºC than in OY. Furthermore, the intermediate $C_{12}A_7$ is also much smaller in CY than in OY. Consequently, it can be assumed that the addition of dopants has decrease the temperature of all the reactions proposed before. Moreover, the presence of SiO_2 may have yield to the formation of intermediate silicates through reactions (12) and (13), although only reaction (13) seems to have taken place since a small amount of belite has been quantified, Figure 7.

$$2CaO + Al_2O_3 + SiO_2 \xrightarrow{<900°C} C_2AS \quad (12)$$

$$2CaO + SiO_2 \xrightarrow{<900°C} C_2S \quad (13)$$

The greater content of ye'elimite in the synthesized materials at 1300°C (OY) and 1250°C (CY) can be favored not only the precise reactants and their chemical purity but by the greater sulphate content present in the raw mix, this sulphate has been reported as a stabilizer of ye'elimite [50].

3.6. Kinetic Model

Base on Jander's model (geometrical and diffusional model), the adjustment of kinetic data is verified on both orthorhombic and cubic ye'elimite. By describing the kinetics of CY and OY, the coexistence of two polymorphs was verified, the activation energy and the rate constant give information about the temperature and residence time tunning up during clinker to favor the formation of OY or CY in CSA.

Temperature highly influences the rate of every chemical reaction. In general, the reaction rate on solid state reactions increases markedly with temperature [51]. As described above, the coexistence of OY and CY was found during the synthesis, however it was possible to identify each of them but mineralogical analysis. We can say that in this research two ye'elimite polymorph have been synthetized successfully and quantified by RQPA including the ACn content in order to find the kinetics of each one and at the end favoring the presence of one or other after sintering process.

In solid state reactions, generally, rate coefficients almost invariably fit one or other form of the Arrhenius equation:

$$k = A \cdot exp^{\left(-\frac{Ea}{RT}\right)} \quad (14)$$

Ea, activation energy, represents the needed energy that must be overcome during the reaction process to transform the reactants into products, i.e., ye'elimite. From (14) is noticeable that the larger the Ea/RT ratio, the smaller the rate. Therefore, in order to determine the Ea of each reaction, i.e., OY and CY formation, linearization of (14) was made by taking the logarithms and separating the terms (exponential Ea/RT and pre-exponential A). Equation (15) is the linear expression allowing to get the Ea, A by the linearity of ln(k) vs 1/T.

Corresponding author: *Jorge I. Tobón. E-mail: jitobon@unal.edu.co

$$\ln k = \ln A - \frac{E_a}{RT} \quad (15)$$

By checking the graphical relationship between the rate coefficient logarithm ln(k) and temperature 1/T, the next step is to identify the best lineal adjustment, which confirms the best kinetic description from polymorphs synthesis. Figure 8 and Figure 9 show, after the fitting Jander's model for both polymorphs (OY an CY respectively), the consequent agreement with Arrhenius formula (16), which represents the temperature dependence of the reactants to proceed with the reaction. From this figure it is possible to get the accumulation factor, A, determined by calculating the inverse of the natural logarithm in the x axe-intercept of the linear adjustment of ln(k) vs 1/T, the rate coefficient, k, determined by calculating the inverse of the natural logarithm in the y axe-intercept of the linear adjustment of ln(k) vs 1/T and the Activation Energy, Ea, determined by the slope of the linear adjustment of the plot ln(k) vs 1/T.

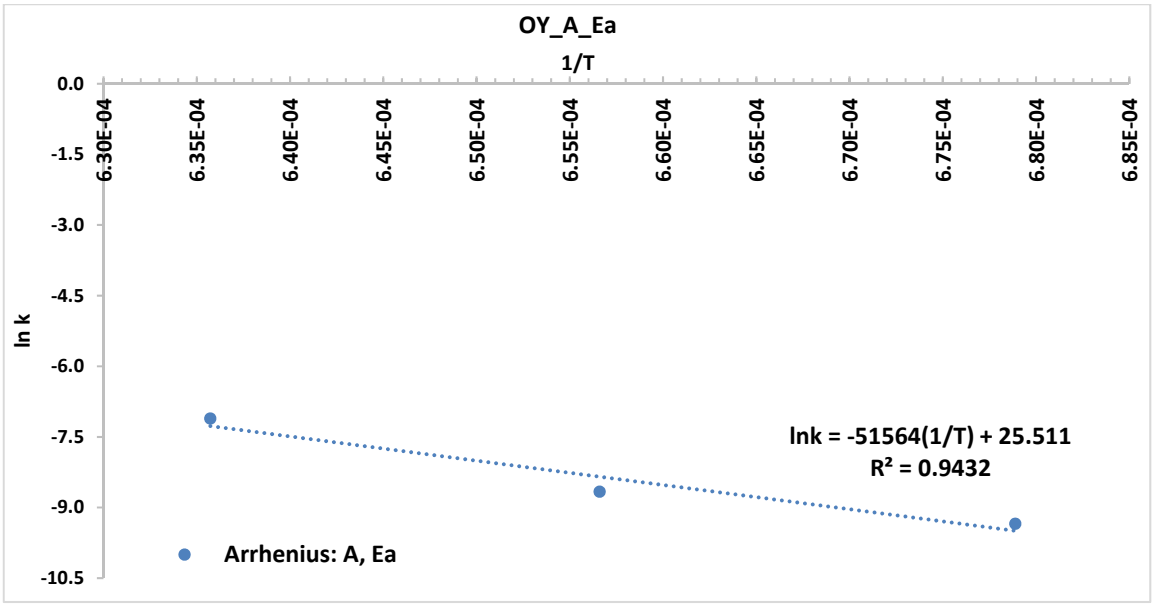

Figure 8. Arrhenius's fitting for OY at different temperatures.

Corresponding author: *Jorge I. Tobón. E-mail: jitobon@unal.edu.co

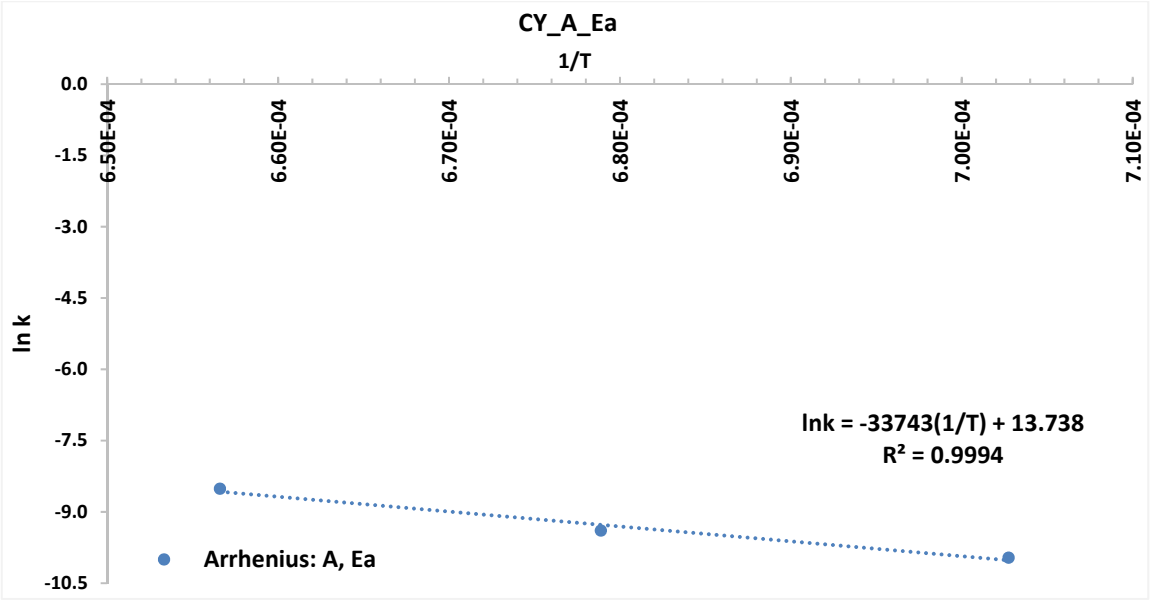

Figure 9. Arrhenius's fitting for CY at different temperatures.

Both polymorphs have a good fitting with diffusional and geometric kinetic model base on Jander (D3). Arrhenius fit gives the kinetic parameters which agree with preliminary thermal analysis. The Arrhenius fitting is better for CY than for OY according to R^2, 0.94 in OY and 0.99 in CY), although both are good enough for this kinetic model. The OY linear slope is higher than CY, it means a higher Ea for OY formation. The addition of minor elements (Table 1) for the stabilization of CY helps to synthetize this polymorph at lower temperature and demanding less energy, Ea.

Table 4. kinetic parameters of OY and CY according to Jander's model

Sample	1/T (K)	k (1/s)	A (1/s)	Ea (kJ/mol)
OY_1200	0.0006789	0.0000876		
OY_1250	0.0006566	0.0001731	1.20E+11	419.94
OY_1300	0.0006357	0.0008190		
CY_1150	0.0007027	0.0000471		
CY_1200	0.0006789	0.0001018	9.25E+05	274.80
CY_1250	0.0006566	0.0002235		

Table 4 summarizes the kinetic parameters of OY and CY obtained by Jander's model. Regarding the frequency factor, A (the pre-exponential factor), is on the normal range [52] compared to the limits for that parameter in a solid state reaction of crystalline compounds. The factor A usually was considered as the frequency of occurrence of the high energy reaction configuration as a molecular encounter or collision, but also is considered as a specific vibration in the reaction coordinate. Therefore, A is a proportional factor which can correlate the temperature with the reaction rate constant. This way, following Arrhenius (14), when the Activation Energy increases in a reaction, the pre-exponential factor increases to maintain the reaction rate constant, meaning that the particles probability of collide increases when temperature increases to maintain the reaction rate at a particular temperature.

Confirmed by the correlation data and the fitness, the linear fitness of a model which better represents the kinetic behavior of OY and CY is the Jander's model. As mentioned before, this model combines

Corresponding author: *Jorge I. Tobón. E-mail: jitobon@unal.edu.co

the geometrical and diffusional phenomenal to describe the ye'elimite formation throughout the solid-to-solid state reaction. The temperatures range was from 1150°C to 1300°C, in that interval, which is the typical sintering temperature at industrial level, this kinetic model is valid.

Figure 10 shows α, equation (1), *vs.* residence time curves for both OY and CY at different temperatures. These curves are useful because they show that there is an adequately representation of the progressive changes in the conversion factor at the temperature working interval used. The shape of those curves represents the rapid onset of an acceleration reaction section. The induction period was not evident on those curves, but it could occur when the majority oxides start to react, i.e., over 1000°C, equation (8).

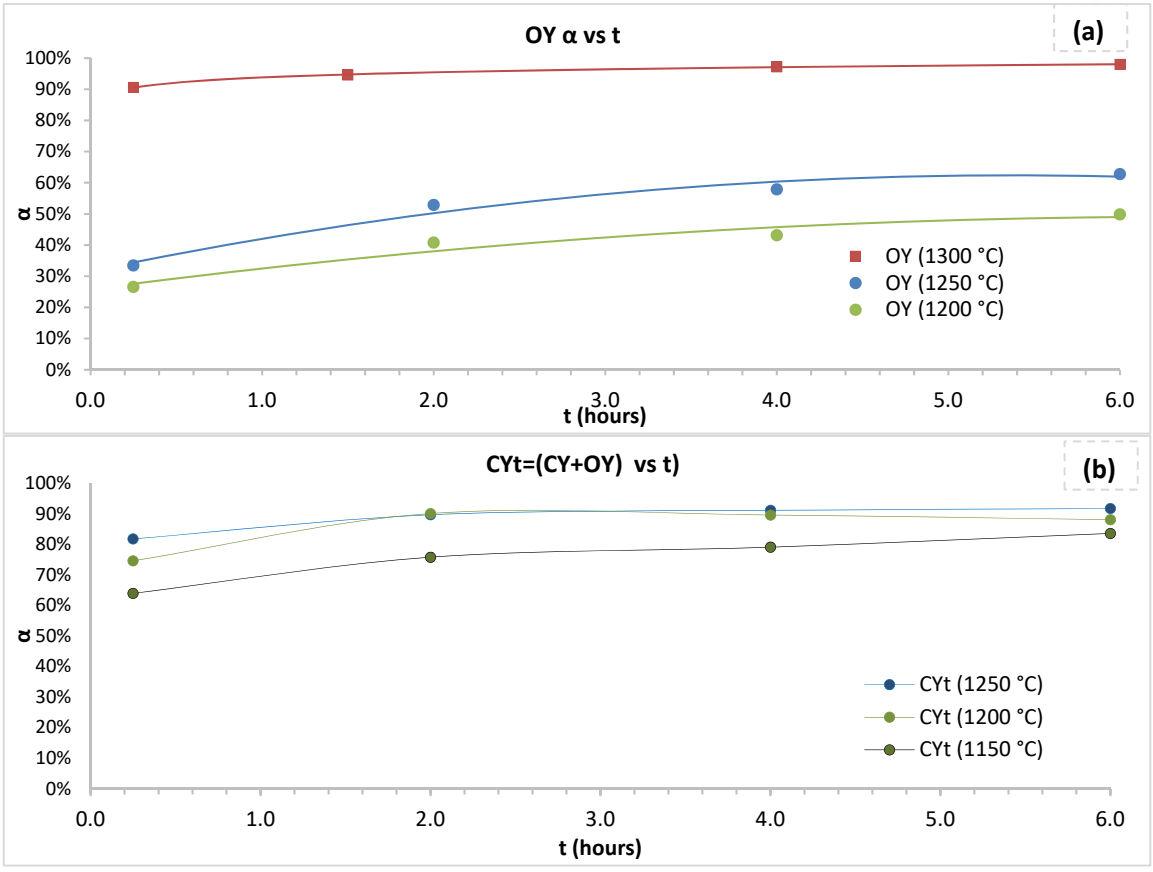

Figure 10. α *vs.* time curve for OY (a) and CY (b) at different temperatures.

Figure 11 represents an additional correlation between the α *vs.* time curve considering the content of OY identified during the CY reaction process. At the beginning OY is the first and most abundant phase in the reaction process, and CY is stabilized at higher temperatures. Therefore, less OY is detected when the reaction formation of CY moves forward with temperature and due to the minor elements used to stabilize de CY. Progressive transformation occurs from OY to CY during the metastable phases equilibrium until getting the maximum CY. Similarly to Figure 10, the shape of those curves represent the rapid onset of an acceleratory reaction section, the induction period is not evident on those curves, it occurred when the majority oxides start to react (over 1000°C, equation (8)), but a OY quantity reduction is noticeable due to the presence of minor elements that transform OY to CY at higher temperature and residence time. It is noticeable how the OY in CY reaction formation diminishes as time and temperature increase. A particular case on OYcu (1150 C), where

Corresponding author: *Jorge I. Tobón. E-mail: jitobon@unal.edu.co

the transition from OY to CY is not as high as at higher temperatures, but CY continue growing up, it is due to slow reaction process at low temperatures for CY formation.

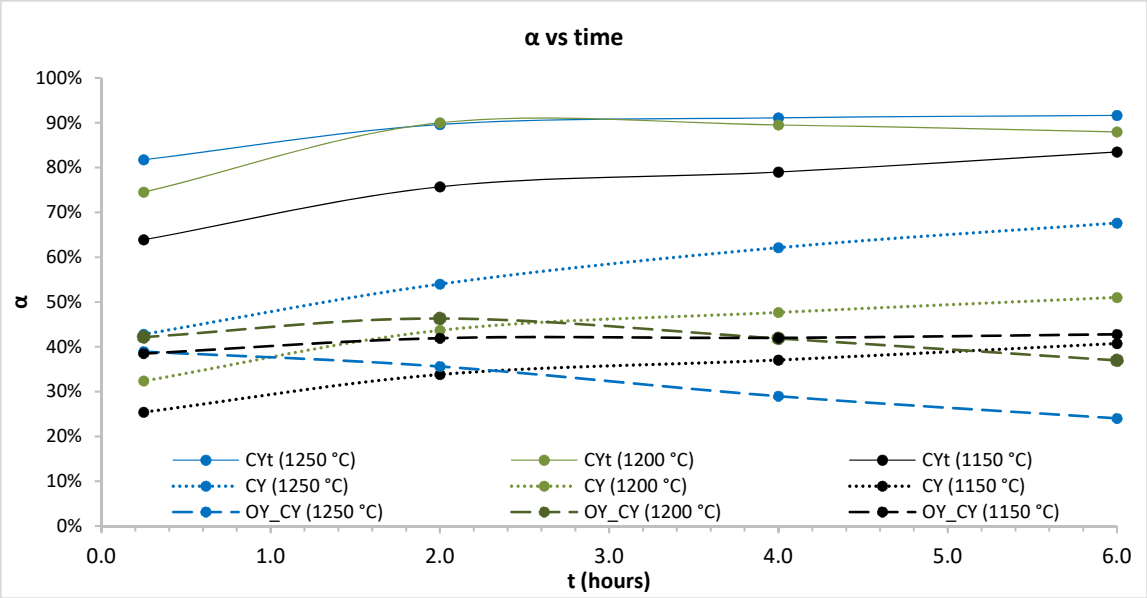

Figure 11. α *vs.* time curve for the orthorhombic presence, OY, in CY sample at different temperatures.

However, it seems that the reaction cannot be analyzed as independent parameters. Consequently, a modified α has been defined to correlate the presence of CY base on the initial OY formation:

$$\alpha_{modified} = (\alpha_{CY})/(\alpha_{CY}-\alpha_{OY}) \quad (16)$$

Figure 12 represents the $\alpha_{modified}$ *vs.* time. On this scenario CY formation, during the evaluated period, depends on the OY transformation to CY. Here CY formation, considering $\alpha_{modified}$, seems to occur slower due to the OY transformation to CY but in higher proportion regarding CY formation by considering α. As on the other ones the shape of those curves represents the acceleration reaction of the experimental α *vs.* time relationship.

Corresponding author: *Jorge I. Tobón. E-mail: jitobon@unal.edu.co

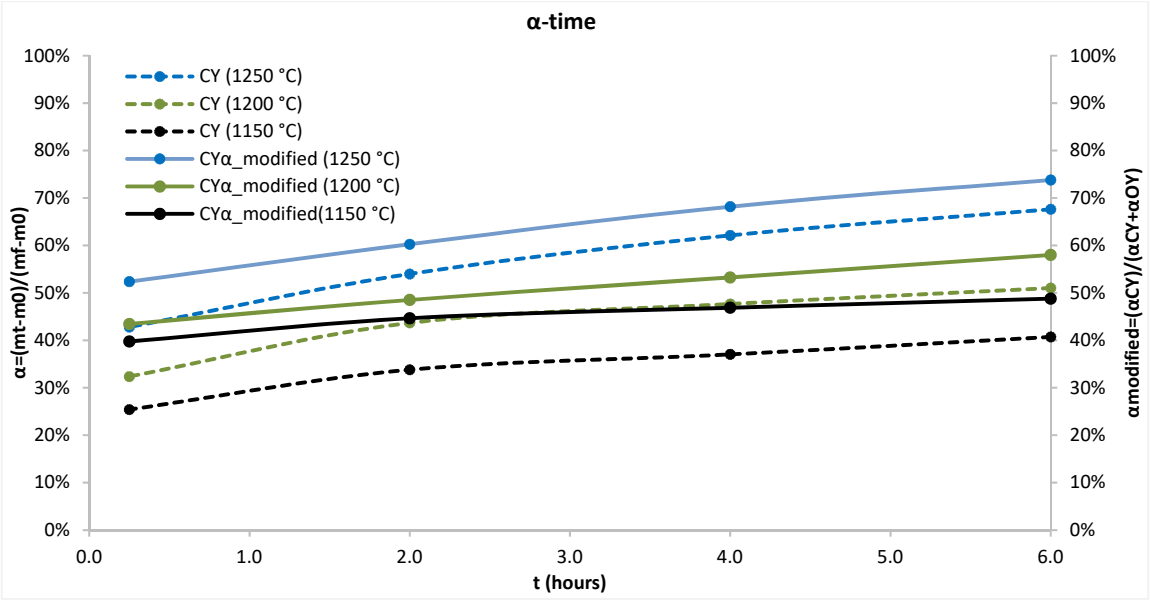

Figure 12. α- time curve, for CY regarding the orthorhombic, OY, presence in CY at different temperatures, varying the conversion factor, α to $\alpha_{modified}$ (equation 16).

According to these results the Jander's diffusional kinetic model fits the kinetics of OY and CY. The kinetic model gives that a higher activation energy is required to get the crystalline form OY than for CY, it is necessary more energy to stabilize and complete the OY reaction rather than CY reaction which means that the kinetic constant increases faster with a temperature changes in OY, and the frequency factor too, which explains that at the same reaction temperature, the more energy and more collisions probability of particles are necessary to form OY. The higher the activation energy the slower the rate reaction. The modified conversion factor $\alpha_{modified}$ shows the relationship between both OY an CY presence during different residence times. From the conversion factor graphs, α vs. time, is showed a kinetic on the temperature interval analyzed during the different residence times describes de diffusional model D3, Jander's model, confirming the model adjustment.

In CY synthesis participates other fundamental components acting as mineralizer and/or net modifiers are the key on CY synthesis, even this work do not develop that chemical approximation, the base of the kinetic difference between CY and OY is based on that. Furthermore, a hypothetical chemical reaction to reach that CY composition by sintering is describe here [35]:

$$\frac{29}{10}CaO + \frac{28}{10}Al_2O_3 + CaSO_4 + \frac{1}{10}Na_2O + \frac{1}{10}Fe_2O_3 + \frac{2}{10}SiO_2 \rightarrow$$
$$(SiO_2)_{0.2}(Na_2O)_{0.1}.(CaO)_{3.9}\,(Al_2O_3)_{2.8}(Fe_2O_3)_{0.1}SO_3 = \frac{1}{5}Ca_{19}NaFeAl_{28}SiSO_{80}$$

4. CONCLUSIONS

It has been found that reaction rate on OY an CY is mainly influenced by geometrical changes and diffusional transport phenomena. The conversion factor, α, versus time curves corresponds to a diffusional model for both, OY and CY. The diffusional models are appropriated to describe the kinetic rate reaction of both, orthorhombic (OY) and cubic (CY) ye'elimite.

Corresponding author: *Jorge I. Tobón. E-mail: jitobon@unal.edu.co

The approximation mathematical model is founded from the Arrhenius expressions. The experimental isothermal conversion factors fix very well by using linear regression calculation (R^2 higher than 94). It has been shown that the kinetic model describes the formation of each polymorph appropriately.

The formation kinetic of both OY and CY is controlled by diffusional oxides moving through the geometry of the particles, mainly from CaO coming from $CaCO_3$, as determined by Jander's model. The activation energies for these models were obtained, being Ea =420 kJ/mol for OY and 275 kJ/mol for CY. The activation energy is lower in CY due to the presence of minor elements that reduce the sintering temperature.

Similarly, the frequency factor or compensation factor A is higher for OY than CY, meaning the need of higher collision frequency. In the same line, the kinetic constant is higher in OY than CY, which agrees with the differences on reaction rate.

The coexistence between OY and CY during the very beginning of CY reaction allows to introduce the $\alpha_{modified}$ which represents better the relationship between the isothermal CY formation trough the time. OY always is present at the reaction beginning. But as higher the temperature and reaction time, in the presence of some minor elements, CY appears mainly at lower temperatures regarding OY, it means requiring lesser energy. Due to the modified structure reached by the CY, different hydration behavior is expected in a CSA cement where CY ye'elimite is mainly present.

Funding: The stay at University of Malaga of A. Berrio was partially funded by Spanish Junta de Andalucía [UMA18-FEDERJA-095] research project, which is cofounded by ERDF.

3. References

[1] M. A. G. Aranda and A. G. De la Torre, "18 - Sulfoaluminate cement," in *Eco-Efficient Concrete*, Elsevier, 2013, pp. 488–522.

[2] L. Zhang and F. P. Glasser, "Investigation of the microstructure and carbonation of CS̄A-based concretes removed from service," *Cem. Concr. Res.*, vol. 35, pp. 2252–2260, 2005, doi: 10.1016/j.cemconres.2004.08.007.

[3] K. L. Scrivener, V. M. John, and E. M. Gartner, "Eco-efficient cements: Potential economically viable solutions for a low-CO2 cement-based materials industry," *Cem. Concr. Res.*, vol. 114, pp. 2–26, Dec. 2018, doi: 10.1016/j.cemconres.2018.03.015.

[4] J. Péra and J. Ambroise, "New applications of calcium sulfoaluminate cement," *Cem. Concr. Res.*, vol. 34, no. 4, pp. 671–676, 2004, doi: 10.1016/j.cemconres.2003.10.019.

[5] M. C. Martín-Sedeño *et al.*, "Aluminum-rich belite sulfoaluminate cements: Clinkering and early age hydration," *Cem. Concr. Res.*, vol. 40, no. 3, pp. 359–369, Mar. 2010, doi: 10.1016/j.cemconres.2009.11.003.

[6] K. L. Scrivener, V. M. John, and E. M. Gartner, "Eco-efficient cements: Potential economically viable solutions for a low-CO2 cement-based materials industry," *Cem. Concr. Res.*, vol. 114, no. March, pp. 2–26, Dec. 2018, doi: 10.1016/j.cemconres.2018.03.015.

[7] C. W. Hargis, A. P. Kirchheim, P. J. M. Monteiro, and E. M. Gartner, "Early age hydration of calcium sulfoaluminate (synthetic ye'elimite, C4A3S̄) in the presence of gypsum and varying amounts of calcium hydroxide," *Cem. Concr. Res.*, vol. 48, pp. 105–115, Jun. 2013, doi: 10.1016/j.cemconres.2013.03.001.

Corresponding author: *Jorge I. Tobón. E-mail: jitobon@unal.edu.co

[8] E. Gartner and T. Sui, “Alternative cement clinkers,” *Cem. Concr. Res.*, vol. 114, pp. 27–39, 2018, doi: 10.1016/j.cemconres.2017.02.002.

[9] Y. Al Horr, A. Elhoweris, and E. Elsarrag, “The development of a novel process for the production of calcium sulfoaluminate,” *Int. J. Sustain. Built Environ.*, vol. 6, no. 2, pp. 734–741, Dec. 2017, doi: 10.1016/j.ijsbe.2017.12.009.

[10] M. Ben Haha, F. Winnefeld, and A. Pisch, “Advances in understanding ye’elimite-rich cements,” *Cem. Concr. Res.*, vol. 123, p. 105778, Sep. 2019, doi: 10.1016/j.cemconres.2019.105778.

[11] E. Gartner, “Industrially interesting approaches to ‘low-CO2’ cements,” *Cem. Concr. Res.*, vol. 34, no. 9, pp. 1489–1498, Sep. 2004, doi: 10.1016/j.cemconres.2004.01.021.

[12] D. Londono-Zuluaga, J. I. Tobón, M. A. G. Aranda, I. Santacruz, and A. G. De la Torre, “Clinkering and hydration of belite-alite-ye´elimite cement,” *Cem. Concr. Compos.*, vol. 80, pp. 333–341, Jul. 2017, doi: 10.1016/j.cemconcomp.2017.04.002.

[13] A. Rungchet, P. Chindaprasirt, S. Wansom, and K. Pimraksa, “Hydrothermal synthesis of calcium sulfoaluminate–belite cement from industrial waste materials,” *J. Clean. Prod.*, vol. 115, pp. 273–283, Mar. 2016, doi: 10.1016/j.jclepro.2015.12.068.

[14] H. N. Yoon, J. Seo, S. Kim, H. K. Lee, and S. Park, “Hydration of calcium sulfoaluminate cement blended with blast-furnace slag,” *Constr. Build. Mater.*, vol. 268, no. xxxx, p. 121214, Jan. 2021, doi: 10.1016/j.conbuildmat.2020.121214.

[15] W. Hou, F. He, and Z. Liu, “Characterization methods for sulfate ions diffusion coefficient in calcium sulphoaluminate mortar based on AC impedance spectroscopy,” *Constr. Build. Mater.*, vol. 289, p. 123169, Jun. 2021, doi: 10.1016/j.conbuildmat.2021.123169.

[16] D. Koumpouri, I. Karatasios, V. Psycharis, I. G. Giannakopoulos, M. S. Katsiotis, and V. Kilikoglou, “Effect of clinkering conditions on phase evolution and microstructure of Belite Calcium-Sulpho-Aluminate cement clinker,” *Cem. Concr. Res.*, vol. 147, no. December 2020, p. 106529, Sep. 2021, doi: 10.1016/j.cemconres.2021.106529.

[17] G. Álvarez-Pinazo *et al.*, “In-situ early-age hydration study of sulfobelite cements by synchrotron powder diffraction,” *Cem. Concr. Res.*, vol. 56, pp. 12–19, 2014, doi: 10.1016/j.cemconres.2013.10.009.

[18] A. Cuesta, G. Álvarez-Pinazo, S. G. Sanfélix, I. Peral, M. A. G. Aranda, and A. G. De la Torre, “Hydration mechanisms of two polymorphs of synthetic ye’elimite,” *Cem. Concr. Res.*, vol. 63, pp. 127–136, Sep. 2014, doi: 10.1016/j.cemconres.2014.05.010.

[19] A. Telesca, M. Marroccoli, L. Coppola, D. Coffetti, and S. Candamano, “Tartaric acid effects on hydration development and physico-mechanical properties of blended calcium sulphoaluminate cements,” *Cem. Concr. Compos.*, vol. 124, no. June 2020, p. 104275, 2021, doi: 10.1016/j.cemconcomp.2021.104275.

[20] N. Ukrainczyk, N. Franković Mihelj, and J. Šipušić, “Calcium sulfoaluminate eco-cement from industrial waste,” in *Chemical and Biochemical Engineering Quarterly*, 2013, vol. 27, no. 1, pp. 83–93.

[21] A. Berrio and J. I. Tobón, “Calcium sulfoaluminate cement , from laboratory to industrial scale,” *14th Int. Congr. Chem. Cem.*, 2015, [Online]. Available:

Corresponding author: *Jorge I. Tobón. E-mail: jitobon@unal.edu.co

http://www.iccc2015beijing.org/dct/page/1.

[22] S. Khare, M. C. Bannerman, F. P. Glasser, T. Hanein, and M. S. Imbabi, "Pilot scale production of novel calcium sulfoaluminate cement clinkers and development of thermal model," *Chem. Eng. Process. Process Intensif.*, vol. 122, pp. 68–75, Dec. 2017, doi: 10.1016/j.cep.2017.10.006.

[23] E. Bastos, E. D. Rodríguez, S. A. Bernal, J. L. Provis, L. A. Gobbo, and A. Paula, "Production and hydration of calcium sulfoaluminate-belite cements derived from aluminium anodising sludge," vol. 122, pp. 373–383, 2016, doi: 10.1016/j.conbuildmat.2016.06.022.

[24] J. Zhang, X. Guan, H. Li, and X. Liu, "Performance and hydration study of ultra-fine sulfoaluminate cement-based double liquid grouting material," *Constr. Build. Mater.*, vol. 132, pp. 262–270, 2017, doi: 10.1016/j.conbuildmat.2016.11.135.

[25] H. Ludwig and W. Zhang, "Cement and Concrete Research Research review of cement clinker chemistry," *Cem. Concr. Res.*, vol. 78, pp. 24–37, 2015, doi: 10.1016/j.cemconres.2015.05.018.

[26] A. Khawam and D. R. Flanagan, "Solid-State Kinetic Models : Basics and Mathematical Fundamentals," vol. 110, no. 35, pp. 17315–17328, 2006, doi: 10.1021/jp062746a.

[27] X. Li, Y. Zhang, X. Shen, Q. Wang, and Z. Pan, "Kinetics of calcium sulfoaluminate formation from tricalcium aluminate, calcium sulfate and calcium oxide," *Cem. Concr. Res.*, vol. 55, pp. 79–87, Jan. 2014, doi: 10.1016/j.cemconres.2013.10.006.

[28] F. Puertas, M. T. B. Varela, and S. G. Molina, "Kinetics of the thermal decomposition of C4A3S̄ in air," *Cem. Concr. Res.*, vol. 25, no. 3, pp. 572–580, Apr. 1995, doi: 10.1016/0008-8846(95)00046-F.

[29] M. M. Ali, S. Gopal, and S. K. Handoo, "STUDIES ON THE FORMATION KINETICS OF CALCIUM SULPHOALUMINATE," *Cem. Concr. Res.*, vol. 24, no. 4, pp. 715–720, 1994.

[30] A. K. Galwey and M. E. Brown, Eds., "Chapter 3: Kinetic models for solid state reactions," in *Thermal Decomposition of Ionic Solids*, 1999, pp. 75–115.

[31] J. Amparo Rodríguez, E. G. Ríos Rodríguez, E. Rocha Rangel, J. M. Almanza Robles, J. Torres, and E. Refugio García, "Kinetics of Formation and Crystal Structure Determination of Sr4Al6O12SO4," *Mater. Res.*, vol. 19, no. suppl 1, pp. 125–132, Feb. 2017, doi: 10.1590/1980-5373-mr-2016-0639.

[32] J. Zhao and J. Chang, "Kinetic Analysis for Formation Process of Sr-Bearing Ye'elimite," *J. Inorg. Organomet. Polym. Mater.*, vol. 27, no. 6, pp. 1861–1869, Nov. 2017, doi: 10.1007/s10904-017-0653-2.

[33] A. Cuesta *et al.*, "Structure, atomistic simulations, and phase transition of stoichiometric yeelimite," *Chem. Mater.*, vol. 25, no. 9, pp. 1680–1687, 2013, doi: 10.1021/cm400129z.

[34] V. JOHANSEN, "Model for Reaction Between CaO Particles and Portland Cement Clinker," *J. Am. Ceram. Soc.*, vol. 56, no. 9, pp. 450–454, 1973, doi: 10.1111/j.1151-2916.1973.tb12521.x.

[35] A. Cuesta, Á. G. De la Torre, E. R. Losilla, I. Santacruz, and M. A. G. Aranda, "Pseudocubic Crystal Structure and Phase Transition in Doped Ye'elimite," *Cryst. Growth Des.*, vol. 14, no.

Corresponding author: *Jorge I. Tobón. E-mail: jitobon@unal.edu.co

10, pp. 5158–5163, Oct. 2014, doi: 10.1021/cg501290q.

[36] A. Berrio, C. Rodriguez, and J. I. Tobón, “Effect of Al2O3/SiO2 ratio on ye’elimite production on CSA cement,” *Constr. Build. Mater.*, vol. 168, pp. 512–521, Apr. 2018, doi: 10.1016/j.conbuildmat.2018.02.153.

[37] B. Touzo, A. Gloter, K. Scrivener, T. Füllmann, and G. Walenta, “PHASE COMPOSITION OF 40 % AL 2 O 3 CALCIUM ALUMINATE CEMENTS,” in *11th International Congress on the Chemistry of Cement*, 2003, no. May, pp. 1931–1940.

[38] A. G. De La Torre, S. Bruque, and M. A. G. Aranda, “Rietveld quantitative amorphous content analysis,” *J. Appl. Crystallogr.*, vol. 34, no. 2, pp. 196–202, Apr. 2001, doi: 10.1107/S0021889801002485.

[39] R. B. Von Dreele and A. C. Larson, “General structure analysis system (GSAS),” *Los Alamos Natl. Lab. Rep. LAUR*, vol. 748, pp. 86–748, 2004.

[40] P. Thompson, D. E. Cox, and J. B. Hastings, “Rietveld Refinement of Debye-Scherrer Synchrotron X-ray Data from A1203,” *J. Appl. Crystallogr.*, vol. 20, no. 2, pp. 79–83, 1987, doi: 10.1107/S0021889887087090.

[41] L. W. Finger, D. E. Cox, and A. P. Jephcoat, “A correction for powder diffraction peak asymmetry due to axial divergence,” *J. Appl. Crystallogr.*, vol. 27, no. 6, pp. 892–900, Dec. 1994, doi: 10.1107/S0021889894004218.

[42] W. A. Dollase, “Correction of intensities of preferred orientation in powder diffractometry: application of the march model,” *J. Appl. Crystallogr.*, vol. 19, no. pt 4, pp. 267–272, 1986, doi: 10.1107/S0021889886089458.

[43] F. R. and R. Jean Rouquerol , Philip Llewellyn , Ricardo Navarrete, “Assessing microporosity nitrogen or liquid argon by immersion microcalorimetry into liquid,” *Stud. Surf. Sci. Catal.*, vol. Volume 144, pp. 171–176, 2002, doi: 10.1016/S0167-2991(02)80131-8.

[44] H. Guo and J. Xie, “Thermodynamics and kinetics of calcium sulphoaluminate,” *J. Wuhan Univ. Technol. Sci. Ed.*, vol. 26, no. 4, pp. 719–722, Aug. 2011, doi: 10.1007/s11595-011-0300-7.

[45] C. W. Hargis, J. Moon, B. Lothenbach, F. Winnefeld, H.-R. Wenk, and P. J. M. Monteiro, “Calcium Sulfoaluminate Sodalite (Ca 4 Al 6 O 12 SO 4) Crystal Structure Evaluation and Bulk Modulus Determination,” *J. Am. Ceram. Soc.*, vol. 97, no. 3, pp. 892–898, Mar. 2014, doi: 10.1111/jace.12700.

[46] M. Idrissi, A. Diouri, D. Damidot, J. M. Greneche, M. Talbi, and M. Taibi, “Cement and Concrete Research Characterisation of iron inclusion during the formation of calcium sulfoaluminate phase,” *Cem. Concr. Res.*, vol. 40, no. 8, pp. 1314–1319, 2010, doi: 10.1016/j.cemconres.2010.02.009.

[47] D. Chen, X. Feng, and S. Long, “The influence of ferric oxide on the properties of 3CaO · 3Al2O3 · CaSO4,” *Thermochim. Acta*, vol. 215, pp. 157–169, Feb. 1993, doi: 10.1016/0040-6031(93)80089-S.

[48] O. Andac and F. P. Glasser, “Polymorphism of calcium sulphoaluminate (Ca 4 Al 6 O16·SO 3) and its solid solutions,” *Adv. Cem. Res.*, vol. 6, no. 22, pp. 57–60, Apr. 1994, doi: 10.1680/adcr.1994.6.22.57.

Corresponding author: *Jorge I. Tobón. E-mail: jitobon@unal.edu.co

[49] G. Álvarez-Pinazo *et al.*, "Rietveld quantitative phase analysis of Yeelimite-containing cements," *Cem. Concr. Res.*, vol. 42, no. 7, pp. 960–971, Jul. 2012, doi: 10.1016/j.cemconres.2012.03.018.

[50] P. Arjunan and M. R. Silsbee, "Sulfoaluminate-belite cement from low-calcium fly ash and sulfur-rich and other industrial by-products," *Cem. Concr. Res.*, vol. 29, no. 8, pp. 1305–1311, Aug. 1999, doi: 10.1016/S0008-8846(99)00072-1.

[51] W. E. Brown, D. Dollimore, and A. K. Galwey, "Reactions in the solid state," in *Comprehensive Chemical Kinetics*, vol. 22, C. H. Bamford and C.F.H. Tipper, Eds. Elsevier Scientific Publishing Company, 1980, pp. 1–289.

[52] K. Measurements, T. H. E. Experimental, and R. Various, "Chapter 5 ANALYSIS AND INTERPRETATION OF EXPERIMENTAL KINETIC MEASUREMENTS," in *Studies In Physical and Theoretical Chemistry*, no. ii, 1999, pp. 139–171.

Corresponding author: *Jorge I. Tobón. E-mail: jitobon@unal.edu.co